

UDC 554.544.654.2

**Sb<sub>2</sub>Se<sub>3</sub>-BASED SOLAR CELLS: OBTAINING AND PROPERTIES****Vusala A. Majidzade***Acad. M.Nagiyev Institute of Catalysis and Inorganic Chemistry**National Academy of Sciences of Azerbaijan,**H.Javid ave., 113, AZ 1143, Baku, Azerbaijan,**e-mail: [yuska\\_80@mail.ru](mailto:yuska_80@mail.ru)**Received 17.01.2020**Accepted 11.04.2020*

**Abstract:** As known, Sb<sub>2</sub>Se<sub>3</sub> is an efficient absorption layer in solar cells because of its optical and electric properties. In recent years, the power conversion efficiency of Sb<sub>2</sub>Se<sub>3</sub> thin film solar cells has gradually enhanced. Consequently, the paper provides an extended review of the literature on various technologies for the preparation of the Sb-Se thin-film system from various aqueous and non-aqueous electrolytes and the research into their structure, as well as some optical and electrical properties. Results of research into potentials of co-deposition on various substrates depending upon temperature, pH and electrolyte composition, sources of antimony and selenium, as well as influence of heat treating on nucleation of Sb<sub>2</sub>Se<sub>3</sub> crystals in various atmospheres were also considered.

**Keywords:** electrodeposition, thin films, antimony selenide, structures of crystals, aqueous and non-aqueous solutions

**DOI:** 10.32737/2221-8688-2020-2-181-198

**Introduction**

Antimony selenide - Sb<sub>2</sub>Se<sub>3</sub> is a semiconductor material belonging to the A<sup>V</sup><sub>2</sub>B<sup>VI</sup><sub>3</sub> group, crystallizing in the rhombic configuration of the Pnma space group (62) [1-5]. The first study on its obtaining was published in the 1950s when Sb<sub>2</sub>Se<sub>3</sub> belonging to the same space group of antimony sulfide - Sb<sub>2</sub>S<sub>3</sub>, had been studied and the structural parameters of Sb<sub>2</sub>Se<sub>3</sub> were evaluated. Later on, these data were confirmed by other research groups and as the current standard, the crystal lattice parameters for Sb<sub>2</sub>Se<sub>3</sub> were taken equal to  $a = 1.16330$  nm,  $b = 1.1700$  nm and  $c = 0.39850$  nm.

Over the years, interest in Sb<sub>2</sub>Se<sub>3</sub> has intensified and the number of studies on the synthesis of this compound has doubled over the past decade.

Studies have shown that this material has excellent electrochemical, Opto- and thermoelectric properties. Sb<sub>2</sub>Se<sub>3</sub> shows a direct forbidden band between 1.04 and 1.3 eV and an optical absorption coefficient is above 10<sup>5</sup> cm<sup>-1</sup> in the visible region, support mobility  $\approx 10$  sm<sup>2</sup>V<sup>-1</sup>s<sup>-1</sup> for non-core supports and, support lifetime  $\approx 60$  ns based on transition absorption

spectroscopy. In addition, it found that Sb<sub>2</sub>Se<sub>3</sub> exhibited an extremely large magnetoresistance.

Based on the electrochemical properties, this material was proposed as an anode material for lithium-ion batteries [6] and materials for the storage of hydrogen [7-8]. The optoelectronic properties of the material are used in materials for optical recording, in thermoelectric devices, solar cells, and photoelectrochemical cells. Also, this material is used in catalytic processes [9]. Currently, the best value of the coefficient of power conversion for a thin film based on Sb<sub>2</sub>Se<sub>3</sub> solar cell with the substrate structure /FTO/ZnO/Sb<sub>2</sub>Se<sub>3</sub>/Au is 5.93 %. However, theoretically calculated intervals with an ideal Shockley-Keisser value predicted that the efficiency of Sb<sub>2</sub>Se<sub>3</sub>-based solar cells could exceed 30%. In addition to the efficiency of solar cells, a critical parameter for the development of such devices is the owning cost of their production. Here Sb<sub>2</sub>Se<sub>3</sub> also satisfies the necessary criteria, since antimony and selenium are widespread and rather cheap elements.

Among the technologies for growth of Sb<sub>2</sub>Se<sub>3</sub> thin films, the most widely spread are

thermal evaporation, chemical bath deposition (CBD), adsorption of ionic layers and chemical reaction methods; spray pyrolysis, reactive-pulsed laser deposition (RPLD), electrodeposition, direct-current (DC) magnetron sputtering, a Resistance Heated Floating Zone Furnace, etc.

### **Chemical methods of deposition**

The authors of [10] presented the results of the deposition of thin films of antimony sulfide and antimony selenide from chemical baths containing  $SbCl_3$  and sources of sulfide or selenide ions in the presence of ligands that form soluble complexes with antimony. As substrates, microscope slides were used. The antimony sulfide precipitation solution was prepared in a 200 ml beaker as follows: 1.3 g of  $SbCl_3$  was dissolved in 5 ml of acetone, then 50 ml of pre-cooled to 283 K 1M  $Na_2S_2O_3$  and 145 ml of cold deionized water were added to the solution and mixed well. The deposition of antimony sulfide was carried out at 283K, the deposition time changed from 1 to 4 hours. An antimony selenide bath was prepared in a 100 ml beaker as follows: 1 g of  $SbCl_3$  was dissolved in 37 ml of 1 M sodium citrate, and then 20 ml of ammonia and 24 ml of 0.4 M  $Na_2S_2O_3$  were added to solution, respectively and diluted with water to the 100 ml mark. The substrates were placed in the bath, vertically resting on the wall of the glass. At the end of the deposition, the glass slides are coated with a mirror-reflecting orange-yellow color. The deposition of antimony selenide was carried out at a room temperature for 2 to 5 hours. Resulting films had low crystallinity, and the width of their band gaps was higher than that of bulk samples (for example, 2.2 eV for  $Sb_2S_3$ ). This was due to quantum confinement arising in films with very small crystallite sizes. However, the films after annealing in nitrogen at a temperature of about 623 K showed clearly defined peaks in X-ray diffraction patterns. This work also was examined the formation of new thin-film materials by annealing multilayer thin films with the participation of antimony chalcogenides. This allows the manufacture of thin-film semiconductors involving a wide range of structural, electrical and optical properties suitable for the manufacture of photonic applications applications with a large area. The possibility of obtaining ternary

Natural abundance, low cost of Sb and Se constituent components, non-toxicity, high absorption coefficient and the width of the forbidden band of  $Sb_2Se_3$  make it a very promising universal functional material for the manufacture of highly efficient thin-film solar cells [1-4].

compounds, such as  $CuSbS_2$ , using the method of chemical deposition and thermal annealing after deposition is shown. A solution for the deposition of copper sulfide was prepared by sequentially adding 10 ml of 0.5 M  $CuCl_2 \cdot 2H_2O$ , 850 ml of triethanolamine, 8 ml of 30 %  $NH_4OH$ , 10 ml of 1 M NaOH, 6 ml of 1 M thiourea and 58 ml of deionized water to chemical glass of 100 ml. Glass substrates coated with thin films of antimony sulfide were placed in a copper sulfide bath. Precipitation was carried out at a room temperature for 2 hours.  $Sb_2S_3\text{-}CuS$  films were annealed for 1 hour in a nitrogen atmosphere.

The preparation of thin films of polycrystalline antimony selenide by chemical bath deposition followed by heating thin films at 573 K in selenium vapor was proposed in [11]. The deposition was carried out in three different solutions of various compositions (a), (b) and (c). For the preparation of solution (a), 25 ml of a 0.1 M solution of antimony potassium tartrate was added to 2 ml of 3.7 M 50% triethanolamine, 20 ml 30% ammonia, 10 ml 0.4 M sodium selenosulfate with stirring and the solution was set up to 100 ml volume with deionized water. Solution (b) was prepared by adding 37 ml of a 1M sodium citrate solution to antimony trichloride ( $SbCl_3$ ) with stirring, then 20 ml of 30% ammonia, 24 ml of 0.4 M sodium selenosulfate were added to it and the solution was set up to 100 ml with deionized water. The composition of solution (c) included 500 mg of  $SbCl_3$  dissolved in 2.5 ml of acetone, 20 ml of 1M sodium citrate, 15 ml of 30% aqueous ammonia, 10 ml of 1M sodium thiosulfate, 20 ml of 0.1 M sodium selenosulfate and it was set up to 100 ml with deionized water. It was found that thin films deposited from chemical baths consisting of antimony salts and sodium selenosulfate along with antimony selenide contain the crystalline oxide phase  $Sb_2O_3$ , moreover, the presence of  $Sb_2Se_3$  was not clearly detected in X-ray diffraction patterns

even after heating at a temperature of 573 K in a nitrogen atmosphere. An analysis of the composition showed that the oxide phase of Sb<sub>2</sub>O<sub>3</sub> could comprise half or more of the thin film material. The composition of the films studied by energy-dispersive X-ray diffraction (EDXRD) analysis showed a deficiency of selenium in the composition of the films. The heating of the films at 573 K in the presence of Se released from the Se powder turns the entire film into Sb<sub>2</sub>Se<sub>3</sub>. These films showed an indirect bandgap of 1 - 1.2 eV. The films were photosensitive with a dark conductivity of about  $2 \cdot 10^{-8}$  (Ohm · cm)<sup>-1</sup> and photoconductivity of about  $10^{-6}$  (Ohm · cm)<sup>-1</sup> when illuminated with a tungsten halogen lamp with an intensity of 700 W · m<sup>-2</sup>.

The photoelectrochemical behavior of a thin Sb<sub>2</sub>Se<sub>3</sub> film obtained by chemical deposition from an aqueous solution was studied [12]. To deposit a thin film of antimony selenide, the solution was prepared by mixing potassium antimony tartrate, triethanolamine, and ammonia with a solution of sodium selenosulfate. The substrate was placed horizontally in the solution, and it was revealed that a thin film of the same thickness was deposited on the downstream side of the electrode. The deposition rate was measured by the extraction of the substrate with a deposit at different times. The temperature of solution and the concentration of its main components on the composition and properties of the deposited films were investigated. When studying the effect of pH, deposition was carried out at a room temperature (303 K) in the solutions with different pH values. The short-circuit photocurrent was about 0.45 mA / cm<sup>2</sup>, and the open-circuit potential was 0.37V. The thickness of the deposited film was measured by the difference in weights taken from the assumption where the film density was the same as that of a bulk sample.

The authors of [13] report on the production of high crystallinity Sb<sub>2</sub>Se<sub>3</sub> nanowires (NW<sub>s</sub>) by chemical vapor deposition. The obtained Sb<sub>2</sub>Se<sub>3</sub> nanowires have triangular prism morphology with a range of proportions from 2 to 200, and on a mica substrate with a symmetric lattice orientation. The study of

structure of the films by Raman spectroscopy with an angular resolution developed specifically for determining the orientation of crystals revealed the strong anisotropic properties of NW<sub>s</sub> Sb<sub>2</sub>Se<sub>3</sub>. In addition, NW<sub>s</sub> Sb<sub>2</sub>Se<sub>3</sub>-based photodetectors exhibit a wide spectral range of photo-responses (400–900 nm). Due to the anisotropic structure of NW<sub>s</sub> Sb<sub>2</sub>Se<sub>3</sub>, the device exhibits a polarization-dependent photoresponse. The high crystallinity and excellent anisotropy of NW<sub>s</sub> Sb<sub>2</sub>Se<sub>3</sub> in combination with a controlled composition give these nanowires high potential for creating multifunctional optoelectronic devices.

### Thermal Deposition Methods

A simple solvothermal method has been developed for the fabrication of large-scale single-crystal Sb<sub>2</sub>Se<sub>3</sub> nanowires [14]. The average nanowire diameter was about 100 nm, and the length was from 1 to 2 microns. Optical properties of Sb<sub>2</sub>Se<sub>3</sub> nanowires were studied by solid-state UV-visible absorption spectroscopy; it found that their bandgap (E<sub>g</sub>) was 1.26 eV.

Also, the nanoribbons from Sb<sub>2</sub>Se<sub>3</sub> were obtained by the solvothermal method using antimony chloride (SbCl<sub>3</sub>), tartaric acid (C<sub>4</sub>H<sub>6</sub>O<sub>6</sub>) and metallic selenium powder (Se) as raw material and N, N-dimethylformamide (DMF) as a solvent. The reaction was carried out at 453 K for 4 h. The influence of the reaction conditions on properties of Sb<sub>2</sub>Se<sub>3</sub> nanoribbons was studied and a possible mechanism of their formation proposed. Large-sized single-crystal Sb<sub>2</sub>Se<sub>3</sub> nanowires were also obtained by the solvothermal method. Parameters such as the reaction medium and sources of the main components of single crystals played a determining role in the morphology and uniformity of final products. In addition, by changing the temperature of the reaction medium, Sb<sub>2</sub>Se<sub>3</sub> nanostructures can also be obtained in the form of nanorods with different diameters [15]. Fig.1 shows the absorption spectra of Sb<sub>2</sub>Se<sub>3</sub> nanostructures obtained at various synthesis temperatures. It can be seen from the figure that by increasing the synthesis temperature of Sb<sub>2</sub>Se<sub>3</sub> nanowires, the intensity of absorption peaks increases.

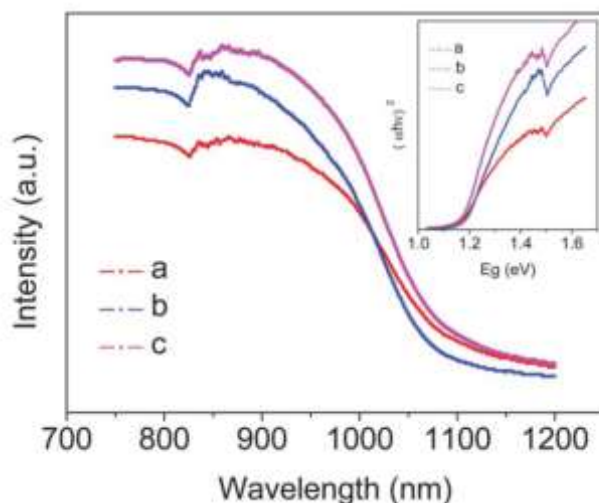


**Fig.1.** Ultraviolet absorption spectra of  $\text{Sb}_2\text{Se}_3$  nanostructures synthesized at various temperatures: (a) 393K, (b) 453K, (c) 493K [15].

The bandgap for the synthesized  $\text{Sb}_2\text{Se}_3$  nanostructures was close in value, optimal for photoelectric converters. This allows suggesting that the synthesized  $\text{Sb}_2\text{Se}_3$  nanostructures can be very promising for applications in solar energy and photo electronics.

One-dimensional rod-shaped  $\text{Sb}_2\text{Se}_3$  nano-compounds were obtained by the solvothermal method at a low temperature (351K). The compound  $[(\text{SbL}_2\text{Cl}_2)\text{Cl}]_2 \times (\text{CH}_3)_2\text{CO}$  (where L is N, N-dimethylselenourea) was used as a source of selenium.

Pure and alloyed antimony selenide crystals ( $\text{Sb}_2\text{Se}_3$ ,  $\text{Sb}_2\text{Se}_{2.8}\text{Te}_{0.2}$ , and  $\text{Sb}_2\text{Se}_{2.6}\text{Te}_{0.4}$ ) were grown from a melt by means of the Bridgman Stockbarger technique. Morphology, microhardness, specific viscosity, brittleness, yield strength, chemical compositions of the compounds were studied, and X-ray diffraction analysis performed [16].

High-quality  $\text{Sb}_2\text{Se}_3$  films were obtained by thermal evaporation using hydrazine as a solvent. Elemental antimony and selenium (molar ratio 1: 3.5) were dissolved in hydrazine and the solution was mixed in a centrifuge for 10 days at a room temperature [17]. It is known that the optimal annealing temperature for grain growth of  $\text{Sb}_2\text{Se}_3$  varied from 673K to 723K. But up to this, the authors carried out the preliminary drying stage at a temperature of 353 K to remove the hydrazine solvent, then soft baking at a temperature of 623

K to evaporate the excess Se, and only then final baking at a temperature of 723 K for the growth of  $\text{Sb}_2\text{Se}_3$  grains. Based on the obtained alloys, a solar cell with a  $\text{TiO}_2/\text{Sb}_2\text{Se}_3$  heterojunction was prepared which achieved a work efficiency of 2.26%. On sodium-calcium glass substrates the synthesis was carried out with heating and without heating the substrates. The films were annealed at various temperatures (373K, 473K, and 573K). X-ray analysis showed that the deposited films without heating the substrate are amorphous, while films grown with simultaneous heating of the substrate are polycrystalline; after annealing, all samples were polycrystalline.

The stable and efficient thin-film solar cells  $\text{CdS} / \text{Sb}_2\text{Se}_3$  were obtained using the process of sublimation in an enclosed space. This allowed the authors to control the temperature of the source and substrate, as well as to reduce interphase diffusion which contributed to improving the quality of the films and improving the heterojunctions of the device [18]. Thin films of antimony selenide were obtained ( $\text{Sb}_2\text{Se}_3$ ) using a simple and fast thermal vapor deposition method (deposition rate  $\sim 1 \mu\text{m} / \text{min}$ ). The crystal growth was oriented perpendicular to the substrate, and thin-film solar cells  $\text{Sb}_2\text{Se}_3$  obtained with a certified device efficiency of 5.6 %. Besides, a technique was developed for the deposition of thin films of antimony selenide of improved crystallinity with vapor transfer which provided the

permanent and inexpensive production of solar cells based on a cadmium sulfide / antimony sulfide substrate with an energy conversion efficiency of 7.6%. Sb-Se semiconductor thin films were obtained on glass substrates from non-aqueous media by spray pyrolysis [19]. The films were deposited from an electrolyte containing antimony trichloride (SbCl<sub>3</sub>) and selenium dioxide (SeO<sub>2</sub>) of the same concentration equal to 0.1 M at various substrate temperatures. At a substrate temperature of 448 K, the film thickness was ~ 0.5 μm. X-ray diffraction studies show that the deposited films at a substrate temperature of 473 K are inherently amorphous, but after annealing in a nitrogen atmosphere at 598 K for two hours become polycrystalline.

Thin films of Sb<sub>2</sub>S<sub>3</sub> and Sb<sub>2</sub>Se<sub>3</sub> with various thicknesses were obtained on Al<sub>2</sub>O<sub>3</sub>, Si, and KCl substrates using pulsed laser ablation. The thickness of the obtained films in a vacuum of 10–5 mm Hg at a substrate temperature of about 453 K was 40–1500 nm. The electrical properties of the films were studied within 253–310 K and it revealed that the films had semiconductor properties [20].

Thin Sb<sub>2</sub>Se<sub>3</sub> films were deposited by thermal evaporation and annealed in a N<sub>2</sub> stream in a three-zone furnace at a temperature of 563 K for 30 min. The deposited film was amorphous, and the annealed film was polycrystalline [21]. The electrical and optical properties of the resulting films were studied. Theoretical calculations carried on by the authors revealed that Sb<sub>2</sub>Se<sub>3</sub> is inherently a semiconductor with an indirect forbidden band.

Crystals (Sn<sub>x</sub>Sb<sub>1-x</sub>)<sub>2</sub>Se<sub>3</sub>, (where x = 0.00, 0.03, 0.05, 0.07, and 0.10) were synthesized using the usual melting method in a vacuum sealing quartz tube [22]. It found that the electrical conductivity of (Sn<sub>x</sub>Sb<sub>1-x</sub>)<sub>2</sub>Se<sub>3</sub> crystals was several orders higher than the conductivity of undoped Sb<sub>2</sub>Se<sub>3</sub> due to a significant increase in the supporting concentration. The dark current density of the sample (Sn<sub>0.10</sub>Sb<sub>0.90</sub>)<sub>2</sub>Se<sub>3</sub> increased by about 10 times, and the photocurrent density by about 14 times. All this, combined with a simple and easy synthesis method, allows the use of this semiconductor for the manufacture of highly efficient photovoltaic devices.

As<sub>14</sub>Ge<sub>14</sub>Se<sub>72-x</sub>Sb<sub>x</sub> films (where x = 3, 6, 9, 12, and 15 at.%) were prepared by thermal evaporation of bulk samples. It found that an increase in the antimony content affected on the refractive index and the attenuation coefficient of the films [23]. In [24], a method for preparing a polycrystalline thin-film Sb<sub>2</sub>Se<sub>3</sub> photocathode with a low bandgap (1.2–1.1 eV) for efficient hydrogen evolution was considered. A thin film was deposited on a substrate of sodium-calcium glass coated with Mo by thermal evaporation of Sb<sub>2</sub>Se<sub>3</sub> powder. Films after annealing under the influence of Se vapors and surface modification with a CdS/TiO<sub>2</sub> anticorrosive layer could be used in the design and manufacture of economical photoelectrochemical cells (RES) operating in a wide range of the solar spectrum. The authors of [25] also used thin antimony selenide films (Sb<sub>2</sub>Se<sub>3</sub>), deposited by the joint process of evaporation of antimony and selenium sources on soda-lime glass coated with molybdenum, to obtain solar cells.

Sb<sub>2</sub>Se<sub>3</sub> films were obtained by melting high-purity Sb and Se (99.999%) with a corresponding weight in a sealed quartz tube at 1123 K in a vacuum for ~ 3 h. It found that Sb<sub>2</sub>Se<sub>3</sub> films had an amorphous structure regardless of thickness, whereas their specific resistances decreased as the melting temperature increased [26]. The optical transmission spectrum showed a very sharp transition near the fundamental absorption edge ~ 1.26 eV [27].

The previously synthesized Sb<sub>2</sub>Se<sub>3</sub> and Sb<sub>2</sub>Se<sub>2</sub>S stoichiometric compositions have been deposited by thermal evaporation on glass substrates. X-ray diffraction studies of annealed at temperatures of 373, 423, and 473 K films showed that the phase transition of the structure from amorphous to crystalline occurs at 423 K and 473 K for Sb<sub>2</sub>Se<sub>3</sub> and Sb<sub>2</sub>Se<sub>2</sub>S, respectively [28].

Thin Sb<sub>2</sub>Se<sub>3</sub> films obtained by vapor deposition were annealed at 473 K in a vacuum for one hour. Comparative evaluations of the properties of films before and after annealing showed that the efficiency of devices designed on the basis of annealed films increased to 5.72 %, while devices with non-annealed films worked with an efficiency of 4.89 % [29]. A significant increase in the efficiency of solar cells (up to 4.8 %) composed of cadmium

sulfide/antimony selenide ( $\text{CdS}/\text{Sb}_2\text{Se}_3$ ) was achieved through controlled addition of oxygen during the thermal evaporation of  $\text{Sb}_2\text{Se}_3$  films [30]. It was shown that the addition of oxygen during evaporation significantly improves the quality of the  $\text{CdS}/\text{Sb}_2\text{Se}_3$  heterojunction.

In [31], to obtain thin  $\text{Sb}_2\text{Se}_3$  films by co-evaporation of Se and  $\text{Sb}_2\text{Se}_3$ , it was proposed to give excess selenium during deposition which led to rise in the concentration of supporting in the  $\text{Sb}_2\text{Se}_3$  absorber. In that case the efficiency of devices using  $\text{Sb}_2\text{Se}_3$  absorber layers increased from 2.1 to 3.47 %.

The chemically deposited thin film [32] of antimony selenide ( $\text{Sb}_2\text{Se}_3$ ) has a coexisting antimony oxide phase ( $\text{Sb}_2\text{O}_3$ ) which can be transformed into crystalline  $\text{Sb}_2\text{Se}_3$  thin films with an optical band gap of 1.13 eV by heating at 280°C in the presence of nitrogen. This leads to the formation of a  $\text{Sb}_2\text{S}_{1.2}\text{Se}_{1.8}$  film with a thickness of 150 nm and with  $E_g = 1.67$  eV. Instead, if heating is carried out with a thin  $\text{Sb}_2\text{S}_3$  film on a chemically deposited  $\text{Sb}_2\text{Se}_3$ :  $\text{Sb}_2\text{O}_3$  thin film, a solid solution is obtained with the coexisting oxide phase  $\text{Sb}_2\text{Se}_{3-z}\text{S}_z$ :  $\text{Sb}_2\text{O}_3$ . The optical band gap of such an absorbing material is 1.34–1.58 eV. Thin deposited films, as well as those obtained by heating, are photoconductive. They were incorporated into solar cell structures developed entirely by chemical deposition of transparent conductive oxide (TCO) glass. Here, the conversion efficiency ( $\eta$ ) is 2.6 %.

$\text{Sb}_2\text{Se}_3$  solar cells were fabricated by thermal evaporation onto a glass substrate coated with fluorine-doped tin oxide (FTO) at various substrate temperatures [33]. A prototype of a multilayer photovoltaic device with a gold contact FTO /  $\text{Sb}_2\text{Se}_3$  /  $\text{CdS}$  /  $\text{ZnO}$  /  $\text{ZnO}$ : Al / Au was designed, which made it possible to achieve a conversion efficiency of solar energy up to 2.1 %.

$\text{Sb}_2\text{Se}_3$  wire microcrystals were synthesized by growth mechanism using a polymer chain of polyethylene glycol (PEG-400) within 433K – 453K temperature for 12–18 h in an autoclave. It was established that pH, reaction temperature, and the use of sodium tartrate are suppliers of the purity of the obtained products [34].

$\text{Sb}_2\text{Se}_3$  nanoribbons were obtained by hydrothermal process at 180°C for 20 hours.

The X-ray diffraction pattern shows that the obtained nanoribbons represent the rhombic phase of  $\text{Sb}_2\text{Se}_3$  with constant lattices  $a=11.747$ ,  $b=11.799$ , and  $c=3.987\text{\AA}$ . Field emission images obtained using a scanning electron microscope show that nanoribbons have a diameter in the range of 25–100 nm and a length of up to 30  $\mu\text{m}$ . The image obtained using high-resolution transmission electron microscopy shows that the nanoribbon was single-crystal and grew on the [001] direction. The absorption peak appeared at 727 nm in the UV-visible spectrum [35].

### Electrochemical deposition methods

Thin  $\text{Sb}_2\text{Se}_3$  films were prepared by electrodeposition, antimony potassium tartrate ( $\text{K}[(\text{C}_4\text{H}_4\text{O}_6)_2\text{SbO}] \cdot 1/2\text{H}_2\text{O}$ ) used as the antimony source, and selenium acid ( $\text{H}_2\text{SeO}_3$ ) in a 0.4M citrate solution was used as selenium source. After annealing at a temperature of 300 ° C in an  $\text{N}_2$  atmosphere, the  $\text{Sb}_2\text{Se}_3$ , Sb, and Se phases were found in the film constitution. Here, the bandgap was 2.00 eV [36]. A thin iron-doped  $\text{Sb}_2\text{Se}_3$  film was obtained by electrodeposition with different amount of iron in film content [37]. It established that the doping agent had a weak effect on the bandgap, morphology, and structural properties of the films, but affected their electronic properties and photoactivity for the release of gaseous hydrogen. Thin polycrystalline  $\text{Sb}_2\text{Se}_3$  films were obtained by electrodeposition from alkaline baths [38]. Triethanolamine (TEA) was used as a complexing agent, and sodium selenosulfide ( $\text{NaSeSO}_3$ ) was the source of the main components. The deposition was carried out in the galvanostatic mode at a room temperature. Resulting thin films were investigated by X-ray diffraction (XRD) and a scanning electron microscope (SEM). A study of the optical absorption of thin  $\text{Sb}_2\text{Se}_3$  films made it possible to determine the bandgap which was 1.14 eV.

In [39], thin three-dimensional (3D)  $\text{Sb}_2\text{Se}_3$  films were synthesized by the electrochemical method on the surface of an ITO electrode in the form of a sandwich-type graphene- $\text{Sb}_2\text{Se}_3$  which significantly improved the photoelectrochemical properties of the films.

The results showed that the bandgap of graphene- $\text{Sb}_2\text{Se}_3$  films in which sheets of reduced graphene oxide were tightly bound to  $\text{Sb}_2\text{Se}_3$  particles, was equal to 1.20 eV.

Homogeneous thin Sb<sub>2</sub>Se<sub>3</sub> films were obtained as a result of their preliminary heat treatment before the usual selenization process [40, 41]. Sources of the films were Sb rich Sb<sub>2</sub>Se<sub>3</sub> deposits obtained by the electrochemical method at a potential of 950 mV.

### 1. charge transfer process

2. wide bandgap E<sub>g</sub> of depletion mode (photoanode with wide E<sub>g</sub> and high Φ<sub>w</sub> value)
3. wide bandgap E<sub>g</sub> mode of weak inversion (photoanode with wide E<sub>g</sub> and low Φ<sub>w</sub>)
4. Narrow bandgap mode of strong inversion, (photoanodes with narrow E<sub>g</sub> and low Φ<sub>w</sub>)

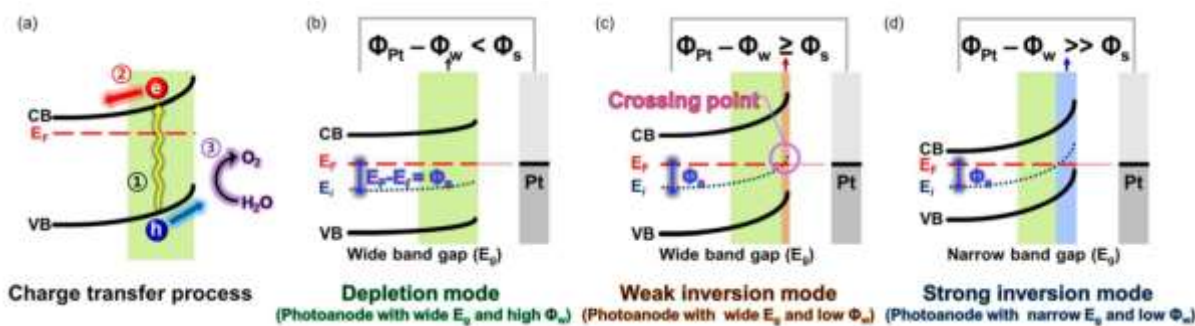


**Fig. 2.** (a) Three-stage photoelectrochemical reaction of water splitting using typical semiconductor photoanodes. Diagrams of the energy zones of the Pt counter electrode and the n-type photoanode before and after electrical contact, where  $\Phi_{Pt}$  = working function of Pt;  $\Phi_w$  = working function of the photoanode; CB = minimum energy of the conduction band;  $E_F$  = Fermi energy level;  $E_i$  = intrinsic energy level; VB = maximum valence band energy:

- (b) the band diagram and the surface depletion region of the photoanode with a wide forbidden zone; the work output is similar to  $\Phi_{Pt}$ ;
- (c) a weak inversion state on the surface of the photoanode with a wide forbidden zone and work output is less than  $\Phi_{Pt}$ ;
- (d) the state of strong inversion on the surface of the photoanode with a narrow bandgap and the work output is much lower than  $\Phi_{Pt}$  [41].

As a result, antimony-rich sources were successfully transformed into thin Sb<sub>2</sub>Se<sub>3</sub> films with improved perpendicular orientation. It is believed that the process of photoelectrochemical splitting of water on typical semiconductor photoelectrodes is carried out through the following three steps as shown in Fig. 2 (a): 1) absorption of light and generation of electron-hole pairs with a higher energy than the bandgap of photo absorbers, 2) separation and migration of photogenerated supporting of charge in the depleted region of the electrode/electrolyte, 3) oxidation/reduction process of water.

The oxygen evolution reaction (OER) occurs at a potential of 1.23 V relative to a reversible hydrogen electrode, a decrease in the efficiency of the semiconductor photoelectrode (photoanode) can lead to bending of the energy zone in equilibrium. The bending of energy zones of the photoelectrodes at the junction

greatly influenced the efficiency of charge separation. In ordinary broadband photoanodes, such as TiO<sub>2</sub>WO<sub>3</sub> and Fe<sub>2</sub>O<sub>3</sub>, the Fermi energy (E<sub>F</sub>) (Fig. 2b) is mainly higher than the average bandgap (intrinsic level, E<sub>i</sub>). Irradiation of photoelectrodes with light does not lead to a decrease in the surface of the band bending caused by photoelectric voltage, i.e., the lower the yield work of the semiconductor photoanodes, the steeper the band bending (Fig. 2 c). Unlike typical oxide photoanodes with a wide bandgap and moderate band bending, photoanodes with a relatively narrow bandgap and low efficiency can provide beneficial situations by effectively absorbing visible and infrared light below 2 eV. The inversion state indicates the transition point at which the surface EF is valued at E<sub>i</sub>, as can be seen from Fig. 1d. In the metal-oxide-semiconductor (MOS) structure, conductive layers or a channel for nonbasic supporting on the

oxide/semiconductor interface provide the inversion state and leads to carrier-type inversions (e.g., p → n or n → p). In the dark state, the depletion region formed on the surface of semiconductor photoelectrodes is naturally formed by the contact with the electrolyte which causes the energy zone to bend and accelerates the charge separation process [41].

Thin films of antimony selenide ( $\text{Sb}_2\text{Se}_3$ ) were prepared on glass substrates coated with  $\text{SnO}_2$  from an acidic aqueous solution by potentiostatic electrodeposition [42]. After annealing at a temperature of 573 K in an Ar atmosphere, the film showed improved crystallinity. It was found that thus obtained  $\text{Sb}_2\text{Se}_3$  films had p-type conductivity and served as good photoelectric converters. Amorphous thin  $\text{Sb}_2\text{Se}_3$  films obtained by electrodeposition from aqueous alkaline electrolytes were proposed as alternative converters of sunlight for semiconductor-sensitized solar cells. After mild thermal annealing in the Ar atmosphere, a phase transition from an amorphous to a crystalline state occurred. The potential of electrodeposited  $\text{Sb}_2\text{Se}_3$  thin films in semiconductor sensitized solar cells was estimated by preparing planar solar cells with a  $\text{TiO}_2/\text{Sb}_2\text{Se}_3/\text{CuSCN}$  heterotransition [43].

Semiconductor thin films of  $\text{Sb}_2\text{Se}_3$  were prepared by electrodeposition on glass substrates coated with tin oxide doped with fluorine from a non-aqueous medium of dimethyl sulfoxide (DMSO). Electrodeposition potentials for various electrolyte compositions were established by taking the polarization curves. Films of good quality are formed from an electrolyte containing  $\text{SbCl}_3$  and  $\text{SeO}_2$  in a volume ratio of 1:1 and with their equimolar solution concentration of 0.03 M [44].

The effect of illumination on the photoelectric deposition of thin  $\text{Sb}_2\text{Se}_3$  films was studied. It was found that the photoconductive effect accelerated the deposition rate of films, and the photogenerated electron (in the conduction band of the deposited thin  $\text{Sb}_2\text{Se}_3$  film) promotes the electroreduction of  $\text{SbO}^+$ . The mechanism of nucleation and growth of semiconductor compounds of antimony selenide ( $\text{Sb}_2\text{Se}_3$ ) on the surface of glass coated with tin oxide doped with indium (indium tin oxide ITO) was studied by chronoamperometry. The electrolysis was carried out at a room

temperature from a nitric acid electrolyte containing both  $\text{Sb}^{3+}$  and  $\text{SeO}_2$  [45]. Antimony and selenium were deposited on the ITO substrate with high overvoltage and diffusion limitations.

A detailed study of the deposition of thin  $\text{Sb}_2\text{Se}_3$  films by the method of electrochemical atomic layer epitaxy (EC-ALE) was performed in [46]. The studies were carried out by the methods of cyclic voltammetry, anodic potentiodynamic polarization scans, and coulometry. It was shown that the deposit is compact and has stoichiometry very close to  $\text{Sb}_2\text{Se}_3$ . A highly productive  $\text{Sb}_2\text{Se}_3$  thin film was obtained by simple low-temperature selenization of electrodeposited antimony [47]. The film was resistant to photo corrosion in strongly acidic media (1M  $\text{H}_2\text{SO}_4$ ); loss over 10 hours was ~ 20%.

Using the methods of cyclic voltammetry (CV) and chronoamperometry (CA), the kinetics of the deposition and dissolution of an antimony monolayer on an Au electrode coated with a Se monolayer was studied [48]. The results show that the formation and dissolution of the monolayer occur as a result of the two-dimensional mechanism of nucleation and growth.

Thin  $\text{Sb}_2\text{Se}_3$  films were deposited by the electrochemical method on matrixes of  $\text{TiO}_2$  nanotubes [49]. Nanotube matrixes prepared in this way showed excellent catalytic properties in the reduction reaction of p-nitrophenol. The electrodeposition mechanism was investigated by electrochemical methods.

In the potentiostatic mode, at a potential of -0.6 V, thin films of antimony selenide were prepared by co-deposition way from an electrolyte of 0.5 M  $\text{Na}_2\text{SO}_4/\text{H}_2\text{SO}_4$  at pH = 2, containing 2.5 mM  $\text{K}(\text{SbO})\text{C}_4\text{H}_4\text{O}_6 \cdot 0.5\text{H}_2\text{O}$  and 2.0 mM  $\text{SeO}_2$  [50]. The films were subjected to heat treatment at various temperatures and heat treatment conditions in an atmosphere of  $\text{Se}(\text{steam})/\text{N}_2$ . The cyclic voltammetry method was used on working electrodes made of Pt and FTO (a glass substrate coated with tin oxide doped with fluorine) to study the electrochemical processes during the deposition of each component separately and in co-deposition. Thin  $\text{Sb}_2\text{Se}_3$  films were electrochemically deposited from an acid-water electrolyte at a room temperature

using selenium dioxide as a source of selenium ions [51]. By taking the polarization curves for different electrolyte compositions, the potentials at which Sb with Se co-electrodeposition occurs was established. It was found that films of good quality are formed at a volume ratio of SbCl<sub>3</sub> and SeO<sub>2</sub> of 9: 1.

Thin films of antimony selenide (Sb<sub>2</sub>Se<sub>3</sub>)

were prepared by potentiostatic electrodeposition on glass substrates coated with SnO<sub>2</sub> from an acidic aqueous solution. The films were then annealed at a temperature of 573 K in an Ar atmosphere. By removing cyclic current-voltage curves, the optimal conditions for the joint electrodeposition of alloy components were found [52].

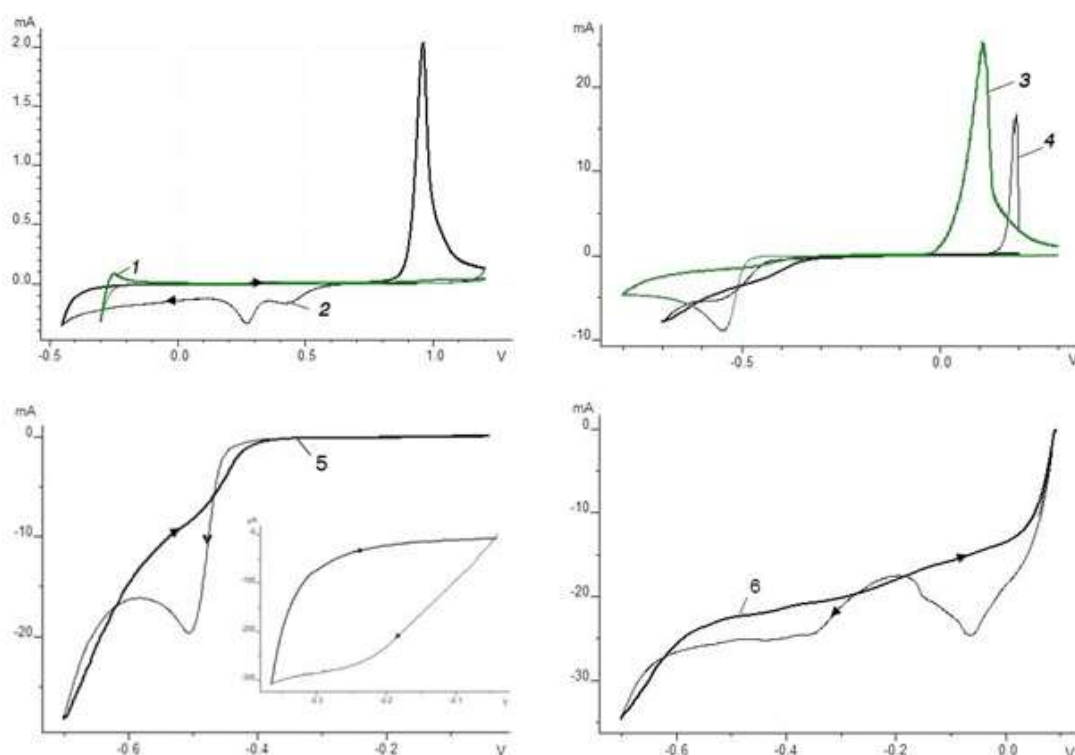


**Fig. 3.** Cyclic polarization curves of electroreduction of selenite, antimony ions and co-deposition of Sb and Se in tartaric acid on different electrodes. The electrolyte composition (M): 1) 0.007 C<sub>4</sub>H<sub>6</sub>O<sub>6</sub> on Pt-electrode; 2) 0.05 H<sub>2</sub>SeO<sub>3</sub> + 0.007 C<sub>4</sub>H<sub>6</sub>O<sub>6</sub> on Pt-electrode; 3) 0.05 SbOCl + 0.007 C<sub>4</sub>H<sub>6</sub>O<sub>6</sub> on Pt-electrode; 4) 0.05 SbOCl + 0.05 H<sub>2</sub>SeO<sub>3</sub> + 0.007 C<sub>4</sub>H<sub>6</sub>O<sub>6</sub> on Pt-electrode; 5) 0.05 SbOCl + 0.05 H<sub>2</sub>SeO<sub>3</sub> + 0.007 C<sub>4</sub>H<sub>6</sub>O<sub>6</sub> on Ni-electrode; 6) 0.05 SbOCl + 0.05 H<sub>2</sub>SeO<sub>3</sub> + 0.007 C<sub>4</sub>H<sub>6</sub>O<sub>6</sub> on Cu-electrode. T = 298 K, v = 0.02 Vs<sup>-1</sup> [52].

A new method for the synthesis of thin Sb<sub>2</sub>Se<sub>3</sub> films that allows changing the morphology of light absorbers proposed. The morphology of Sb<sub>2</sub>Se<sub>3</sub> films can vary from thick particles of flat films to one-dimensional films deposited in nanowires [53]. The method consists of sequential deposition of CdS as a buffer layer with TiO<sub>2</sub> and Pt which allowed creating a favorable range of band structure. A surface-modified photocathode in a neutral electrolyte stably produces hydrogen with a photocurrent of 11 mA/cm<sup>2</sup> at 0.0 V potential relative to a normal hydrogen electrode demonstrating a high potential for using these

photocathodes based on Sb<sub>2</sub>Se<sub>3</sub> as effective devices in the reaction of water splitting. The influence of the concentration ratios of Se/Sb in the solution on the morphology and properties of the obtained Sb<sub>2</sub>Se<sub>3</sub> films was studied.

The work [54] deals with the electrochemical deposition of thin Sb<sub>2</sub>Se<sub>3</sub> films from tartrate electrolytes. The study was conducted by means of potentiodynamic, potentiostatic and galvanostatic methods carried out under various conditions on Pt, Cu and Ni electrodes.

As can be seen from Fig. 3, the electroreduction of selenite ions occurs in steps.

It is known that the standard electrode potential of selenite ions is more positive than the standard electrode potential of antimony ions. This affects the location of the polarization curves and the formation of the  $\text{Sb}_2\text{Se}_3$  compound on the surface of Pt and Ni electrodes occurs between electroreduction potentials of antimony ions (-0.46 V) [55] and selenite ions (0.4 V) [56]. The co-deposition of  $\text{Sb}_2\text{Se}_3$  occurs at a potential of -0.44 V, i.e. the alloy formation is accompanied by depolarization. Starting at -0.44 V, the surfaces of the Pt and Ni electrodes are completely covered by a layer of amorphous Sb-Se which does not occur on the Cu electrode (Fig. 3, curve 6).

The effect of electrolyte composition, pH, current density, temperature, etc. was studied in the course of polarization curves. Based on cyclic polarograms, X-ray phase analysis, and SEM-EDX analysis, it found that thin Sb-Se films are well deposited on the surface of Pt and Ni electrodes, and not deposited on Cu electrodes. Amorphous  $\text{Sb}_2\text{Se}_3$  films of stoichiometric composition were obtained on the surface of Pt and Ni cathodes in the temperature range of 338-348 K, where pH = 1.85, current density 2.5-3.0 A/dm<sup>2</sup>; after annealing at 703K in an argon atmosphere the deposit became polycrystalline.

The influence of various factors, such as temperature, component concentration in the electrolyte, current density on the composition of thin electrodeposited Sb-Se semiconductor films was studied [57]. The results show that the antimony content in the deposited compounds increases with increasing temperature and  $\text{SbOCl}$  concentration. An increase in the current density and concentrations of  $\text{H}_2\text{SeO}_3$  and  $\text{C}_4\text{H}_6\text{O}_6$  leads to a decrease in the antimony content in the resulting thin films. It found that black, uniform, crystalline and shiny thin films of the  $\text{Sb}_2\text{Se}_3$  compound are formed in the temperature range of 298-318K, current densities of 20-60 mA/cm<sup>2</sup> from an electrolyte of the following composition 0.01-0.09 M  $\text{SbOCl}$ , 0.01-0.09 M  $\text{H}_2\text{SeO}_3$  and wine acid 0.001-0.007 M.

### Properties of $\text{Sb}_2\text{Se}_3$ Thin Films

In [58], a method was proposed to increase the efficiency of thin-film solar cells  $\text{Sb}_2\text{Se}_3$  by depositing a monatomic  $\text{Al}_2\text{O}_3$  layer

which leads to an increase in the concentration of the holes in the  $\text{Sb}_2\text{Se}_3$  film. An increase in concentration of the holes is mainly associated with the decline of n-type defects due to the volume concentration of selenium, or an increase in p-type defects due to the volume concentration of antimony. A simple and environmentally friendly oxygen-plasma method was used to modify the CdS film, which allows one to obtain  $\text{Sb}_2\text{Se}_3$  films with an ordered columnar structure. Thus, a solar cell with a new multilayer structure, FTO/CdS/p- $\text{Sb}_2\text{Se}_3/\text{P+}\text{Sb}_2\text{Se}_3/\text{Al}_2\text{O}_3/\text{Au}$ , was prepared, and its efficiency was increased from 2.48% to 6.7%. These simple, non-toxic and industrially applicable methods provide broad opportunities to manufacture low-cost and highly efficient solar cells.

The influence of the conditions of sublimation of  $\text{Sb}_2\text{Se}_3$  films in closed space (close space sublimation-CSS) and their growth parameters have been studied. The obtained  $\text{Sb}_2\text{Se}_3$  films were studied using SEM, XRD, and optical transmission measurements [59]. Photovoltaic devices were fabricated using  $\text{TiO}_2$ .

In [60], new photocathodes and a photoanode were made from antimony and nickel selenide which increase the efficiency of graphene quantum dots of co-sensitized solar cells. Using  $\text{Sb}_2\text{Se}_3$  as an electrode component doubles the properties of the photocathode. It is known that defects in the absorbent layer significantly increase the performance of the photoelectric device. It found that small acceptors, Se-Sb antisites are the dominant defects in  $\text{Sb}_2\text{Se}_3$  which are formed in films with a high Se content [61].

An ultrathin CdS/ $\text{Sb}_2\text{Se}_3$  solar cell was designed to provide an efficiency of up to 5.76%. It is known that in most thin-film based on  $\text{Sb}_2\text{Se}_3$  solar cells, the toxic CdS compound is used as a buffer layer. In [62], non-toxic broadband and chemically stable  $\text{SnO}_2$  was used as a buffer layer to create ultrathin thin-film solar cells  $\text{SnO}_2/\text{Sb}_2\text{Se}_3$  instead of CdS.

The antimony sulfide selenide  $\text{Sb}_2(\text{S}, \text{Se})_3$ , including  $\text{Sb}_2\text{S}_3$  and  $\text{Sb}_2\text{Se}_3$ , can be considered as semiconductors of binary metal chalcogenides since both  $\text{Sb}_2\text{S}_3$  and  $\text{Sb}_2\text{Se}_3$  are isomorphic. Thanks to the study of new-generation thin-film and nanostructured solar

cells, this class of materials was used in flat heterojunction solar cells. The energy conversion efficiency, in this case, increased from 5 % to 7.5 % [63].

The structural and phase transitions, as well as the optical properties of Sb<sub>2</sub>Se<sub>3</sub>:Sn films, were studied in [64]. It found that at the temperature of phase transformation, the resistance in the films decreased by two orders of magnitude. It was observed that the phase transition temperature in thin (Sb<sub>2</sub>Se<sub>3</sub>)<sub>100-x</sub>Sn<sub>x</sub> films increase from 453K for x=0 to 493K for x=5. The structural and optical properties of (Sb<sub>2</sub>Se<sub>3</sub>)<sub>100-x</sub>Sn<sub>x</sub> (x=0.5) films were studied. The results obtained allow the authors to suggest that the addition of Sn leads to an improvement in the optical properties of Sb<sub>2</sub>Se<sub>3</sub> films.

It is known that most A<sub>2</sub>B<sub>3</sub> chalcogenide systems with a strong spin-orbit coupling, such as Bi<sub>2</sub>Se<sub>3</sub>, Bi<sub>2</sub>Te<sub>3</sub>, Sb<sub>2</sub>Te<sub>3</sub>, etc., are topological insulators. The authors of [65] showed that Sb<sub>2</sub>Se<sub>3</sub>, like Bi<sub>2</sub>Se<sub>3</sub> displays the current generation with high spin polarization at mesoscopic superconducting point contacts. The observed high spin polarization and related to its phenomena in Sb<sub>2</sub>Se<sub>3</sub> are explained by the spin splitting of the Rashba type. In addition, a largely negative and anisotropic magnetoresistance was observed in Sb<sub>2</sub>Se<sub>3</sub> films when the field was rotated in the basal plane. Thus, it has been experimentally proved that Sb<sub>2</sub>Se<sub>3</sub> is a regular band insulator, but due to its high spin-orbit coupling, a non-trivial spin-texture forms on the surface.

Chalcogenides of metals based on Ch - M - M - Ch structure (Ch = chalcogen, M = metal) have several attractive properties that make them suitable for use in both electrical and optical devices. The growth of layered InSe and Sb<sub>2</sub>Se<sub>3</sub> semiconductors and their heterostructure have been studied. It has been established that  $\gamma$ -InSe and Sb<sub>2</sub>Se<sub>3</sub> mirror films with a large area can be grown by atomic layer deposition (ALD) method at relatively low temperatures [66].

The main physical properties of Sb<sub>2</sub>Se<sub>3</sub>, such as dielectric constant, anisotropic mobility, carrier lifetime, diffusion length, depth, and density of defects have been studied [67]. The authors concluded that the characterization of the basic physical properties of Sb<sub>2</sub>Se<sub>3</sub> films forms a great basis for further optimization of the operation of a solar device based on them. A

new approach for the fabrication of 1D Sb<sub>2</sub>Se<sub>3</sub> nanostructured arrays (NAs) on conductive substrates by simple coating by centrifugation of Sb-Se solutions with different molar ratios of thioglycolic acid and ethanolamine was proposed in [68]. A relatively small fraction of thioglycolic acid leads to the growth of short Sb<sub>2</sub>Se<sub>3</sub> nanorods, which leads to rapid carrier transfer and an increase in photocurrent.

The carrier dynamics in Sb<sub>2</sub>Se<sub>3</sub> photocathodes for photoelectrochemical water splitting was studied in [69]. These studies were meant to improve the performance of devices for the water splitting based on Sb<sub>2</sub>Se<sub>3</sub> semiconductors.

The photoconductivity spectra of amorphous Sb<sub>2</sub>Se<sub>3</sub> and Sb<sub>2</sub>Se<sub>3</sub>:Sn films [70] were studied where a band was detected due to the presence of defect states with a maximum at 1.46 eV. The intensity of this band in the samples increased as the tin content in the films went up. And in [71], the stationary spectra of the photocurrent of Sb<sub>2</sub>Se<sub>3</sub> and Sb<sub>2</sub>Se<sub>3</sub>:Sn films were studied at photon energies from 1 to 2.5 eV for various values of electric field strength and temperature. The main physical properties of Sb<sub>2</sub>Se<sub>3</sub> films, such as permittivity, anisotropic mobility, carrier lifetime, Debye length, defect depth, defect density, and optical properties were studied in [72]. The effect of defects on the properties of thin-film solar cells based on Sb<sub>2</sub>Se<sub>3</sub> [73] and the influence of various factors on the crystal formation in Sb<sub>2</sub>Se<sub>3</sub> compound were also studied.

The effect of the intensity and duration of photoirradiation on the properties of the amorphous Sb<sub>2</sub>Se<sub>3</sub> film was studied in [74]. It found that after intense and prolonged photoirradiation, both the dark conductivity and the photoconductivity of the films decreased. The thin-film glass-ceramics consisting of a multilayer system: GeSe<sub>2</sub> - Sb<sub>2</sub>Se<sub>3</sub> - CuI was made for photoelectric purposes by sputtering and behaved like a p-type semiconductor, although it contained p-type Cu<sub>2</sub>GeSe<sub>3</sub> and n-type Sb<sub>2</sub>Se<sub>3</sub>. The conductivity of Sb<sub>2</sub>Se<sub>3</sub> was significantly improved due to suitable doping with iodine [75]. The authors studied cleaved samples, topology of surfaces, and electronic structure [76] of thin Sb<sub>2</sub>Se<sub>3</sub> films. This allowed them to obtain information about the electronic properties of Sb<sub>2</sub>Se<sub>3</sub> which is important for

using them as an electrode for photoelectrochemical converters (PEC). It showed that  $\text{Sb}_2\text{Se}_3$  has an indirect bandgap of 1.21 eV.

The optical transmission and reflection of amorphous  $\text{Sb}_x\text{Se}_{1-x}$  thin films where ( $0 \leq x \leq 0.9$ ) of various thicknesses (from 40 to 320 nm) were measured at a room temperature within the wavelength range of 500–1300 nm. From the obtained data, the absorption coefficient, extinction coefficient, refractive index, optical energy gap, and density of states of the valence band for various values were calculated. It was found that these constants did not depend on the film thickness, but noticeably depend on the value of “ $x$ ” [77].

As is known, semiconductor nanostructures with a length of less than 10 nm are crucial for creating nanoscale devices. The authors of [78] established through the calculation that autonomous ribbons of  $\text{Sb}_2\text{Se}_3$  and  $\text{Sb}_2\text{S}_3$  with a width of 1.1 nm had a clearly defined bandgap which was 1.66 and 2.16 eV, respectively. Molecular dynamics studies show that these films are stable at a temperature of 500K.

The main and optical forbidden bands for  $\text{Sb}_2\text{O}_3$ ,  $\text{Sb}_2\text{S}_3$ ,  $\text{Sb}_2\text{Se}_3$ , and  $\text{Sb}_2\text{Te}_3$  thin films were calculated [79]. An analysis of the electron density of states and charge density showed that asymmetric density, or “lone pairs” is formed on Sb (III) cations of distorted oxide, sulfide and selenide materials. Asymmetric density gradually weakens the series due to an increase in the energy of p-valence states from O to Te, and it is absent for  $\text{Sb}_2\text{Te}_3$ . It revealed that  $\text{Sb}_2\text{O}_3$ ,  $\text{Sb}_2\text{S}_3$ , and  $\text{Sb}_2\text{Se}_3$  have indirect forbidden bands, while  $\text{Sb}_2\text{Te}_3$  has a direct forbidden band, and its value decreases from  $\text{Sb}_2\text{O}_3$  to  $\text{Sb}_2\text{Te}_3$ . This optical bandgap makes

$\text{Sb}_2\text{O}_3$  suitable as a transparent conductive oxide while  $\text{Sb}_2\text{S}_3$  and  $\text{Sb}_2\text{Se}_3$ , due to the bandgap, are suitable for preparing thin-film absorbers in solar cells.

The authors of [80] designed the  $\text{Pt}/\text{C}_{60}/\text{TiO}_2/\text{Sb}_2\text{Se}_3$  device which demonstrated higher photocurrent density of  $17\text{mA/cm}^2$  and stability for 10 hours of operation as compared with  $\text{Sb}_2\text{Se}_3$ -based photocathodes. These studies provide a new direction for achieving long-life photocathodes suitable for photoelectrochemical water splitting.

In [81], while preparing  $\text{Sb}_2\text{Se}_3$ -based photocathodes as an effective lower contact layer, a thin  $\text{NiO}_x$  film doped with Cu:  $\text{NiO}_x$  copper was proposed. The introduction of Cu:  $\text{NiO}_x$  blocks recombination at the back boundary, at the same time facilitating hole extraction, at that the photocurrent of  $\text{Sb}_2\text{Se}_3$  photocathode increases to a high-level  $17.5\text{ mA/cm}^2$ . Spectroscopy of electrochemical impedance and spectroscopy of a photocurrent with intensity modulation in combination with other observations show that the photocurrent amplification is due to improved quality of the lower contact without a noticeable change in the upper interface.

Some electrical properties of thin semiconductor  $\text{Sb}_2\text{Se}_3$  films obtained from tartrate electrolytes by electrochemical deposition were studied [82]. Resulting films had n-type conductivity. Some semiconductor constants of the deposited  $\text{Sb}_2\text{Se}_3$  films were determined, such as temperature sensitivity coefficient  $B = 15100\text{ K}$ , temperature coefficient of resistance which was equal to  $\alpha = 0.167\text{ K}^{-1}$  at 300 K and  $\alpha = 0.094\text{ K}^{-1}$  at 400 K. The bandgap was  $E_g = 1.3\text{ eV}$ . Research results showed that thin  $\text{Sb}_2\text{Se}_3$  films can be used in solar energy converters and in thermocouples.

### Conclusions

Here, a brief overview of the main properties of  $\text{Sb}_2\text{Se}_3$  and its corresponding progress in photovoltaic applications are presented. To find the optimal solution, thin films were obtained by various methods on various substrates. Despite the same stoichiometric composition ( $\text{Sb}_2\text{Se}_3$ ), depending on the preparation methods and regimes, the composition of the electrolytic thin films show different properties and characteristics. From

this point of view, the approach to their application in various fields are not the same. An analysis of the literature shows that films obtained on conductive glasses by electrochemical methods demonstrated large absorption coefficient, and high energy conversion efficiency which made it more suitable for thin-film solar cells. In further studies, it'll be necessary to pay attention to the study of fundamental optoelectronic properties

of Sb<sub>2</sub>Se<sub>3</sub>, the systematic optimization of the quality of these films, the efficiency of the solar battery, etc. Given the above, it is possible to

improve efficiency and performance of solar cells based on the promising thin Sb<sub>2</sub>Se<sub>3</sub> film.

### References

1. Zeng K., Xue D.J., Tang J. Antimony selenide thin-film solar cells. *Semicond. Sci. Technol.*, 2016, vol. 31, 063001. . <https://doi.org/10.1088/0268-1242/31/6/063001>
2. Chen C., Bobela D.C., Yang Y., Lu S., Zeng K., Ge C., Yang B., Gao L., Zhao Y., Beard M.C., Tang J. Characterization of basic physical properties of Sb<sub>2</sub>Se<sub>3</sub> and its relevance for photovoltaics. *Front. Optoelectron.*, 2017, vol. 10, pp.18–30.
3. Messina S., Nair M.T.S., Nair P.K. Antimony selenide absorber thin films in allchemically deposited solar cells. *J. Electrochem. Soc.*, 2009, vol. 156, pp. H327–H332.
4. Deringer V.L., Stoffel R.P., Wuttig M., Dronskowski R. Vibrational properties and bonding nature of Sb<sub>2</sub>Se<sub>3</sub> and their implications for chalcogenide materials. *Chem. Sci.*, 2015, issue 9, pp. 5255–5262.
5. Aliyev I.I., Mammadova N.A., Sadigov F.M. Research into phase formation and some physical and chemical properties of the Sb<sub>2</sub>Se<sub>3</sub>-GaSe system alloys. *Chemical Problems*, 2019, vol.17, no.3, pp. 403-407.
6. Patil V., Patil A., Choi J.W., Yoon S.J. Chemically Deposited Sb<sub>2</sub>Se<sub>3</sub> Anode for Thin Film Lithium Batteries. *Journal of Computer Applications for Modeling, Simulation, and Automobile*, 2012, pp. 221–228. <https://doi:10.1007/978-3-642-35248-5>
7. Fateev V.N., Alexeeva O.K., Korobtsev S.V., Seregina E.A., Fateeva T.V., Grigoriev A.S., Aliyev A.Sh. Problems of accumulation and storage of hydrogen. *Chemical Problems*, 2018, vol. 16, no.4, pp. 453 – 483. <https://doi.org/10.32737/2221-8688-2018-4-453-483>
8. Kulova T.L., Nikolaev I.I., Fateev V.N., Aliyev A.Sh. Modern electrochemical systems of energy accumulation. *Chemical Problems*, 2018, vol. 16, no.1, pp. 9–34. <https://doi.org/10.32737/2221-8688-2018-1-9-34>
9. Hu N., Cheney M.A., Hanifehpour Y., Joo S.W., Min B.K. Synthesis, Characterization, and Catalytic Performance of Sb<sub>2</sub>Se<sub>3</sub> Nanorods. *J. Nanomater.*, 2017, Article ID 5385908. (8) <https://doi.org/10.1155/2017/5385908>
10. Rodríguez-Lazcano Y., Guerrero L., Gomez Daza O., Nair M.T.S., Nair P.K. Antimony chalcogenide thin films: chemical bath deposition and formation of new materials by post deposition thermal processing. *Superficies y Vacío*, 1999, no. 9, pp. 100-103.
11. Rodríguez-Lazcano Y., Pena Y., Nair M.T.S., Nair P.K. Polycrystalline thin films of antimony selenide via chemical bath deposit ion and post deposit ion treatments. *Thin Solid Films*, 2005, vol. 493, pp. 77 – 82.
12. Bhattacharya R.N., Pramanik P. A photoelectrochemical cell based on chemically deposited Sb<sub>2</sub>Se<sub>3</sub> thin film electrode and dependence of deposition on various parameters. *Sol. Energy Mater.*, 1982, no. 6, pp. 317-322.
13. Ma Z., Chai Sh., Feng Q., Li L., Li X., Huang L., Liu D., Sun J., Jiang R., Zhai T., Xu H. Chemical Vapor Deposition Growth of High Crystallinity Sb<sub>2</sub>Se<sub>3</sub> Nanowire with Strong Anisotropy for Near-Infrared. *Small*, 2019, vol. 15, issue 9, 1805307. <https://doi:10.1002/smll.201805307>.
14. Sun Sh., Xing Y., Jin R. Synthesis and Optical Property of Sb<sub>2</sub>Se<sub>3</sub> Nanowires. *J. Nanosci. Nanotechnol.*, 2013, vol.13, pp. 5910–5913.
15. Ma J., Wang Y., Wang Y., Peng P., Lian J., Duan X., Liu Z., Liu X., Chen Q., Kim T., Yao G., Zheng W. One-dimensional Sb<sub>2</sub>Se<sub>3</sub> nanostructures: solvothermal synthesis, growth mechanism, optical and electrochemical properties. *CrystEngComm*, 2011, vol.13, no.7, pp. 2369–2374.
16. Chandrasekharan K.A., Kunjomana A.G. Growth and microindentation analysis of pure and doped Sb<sub>2</sub>Se<sub>3</sub> crystals. *Turk. J. Phys.*, 2009, vol. 33, no.4, pp. 209-217. 17. Zhou Y., Leng M., Xia Z., Zhong J., Song H., Liu X., Yang B., Zhang J., Chen J.,

- Zhou K., Han J., Cheng Y., Tang J. Solution-processed antimony selenide heterojunction solar cells. *Adv. Energy Mater.*, 2014, vol. 4, no. 8, pp. 1079–1083.
18. Li D., Yin X., Grice C.R., Guan L., Song Z., Wang Ch., Chen Ch., Li K., Cimaroli A.J., Awani R.A., Zhao D., Song H., Tang W., Yan Y., Tang J. Stable and Efficient CdS/Sb<sub>2</sub>Se<sub>3</sub> Solar Cells Prepared by Scalable Close Space Sublimation. *Nano Energy*, 2018, vol. 49, pp. 346-353.
19. Rajpure K.Y., Lokhande C.D., Bhosale C.H. Effect of the substrate temperature on the properties of spray deposited Sb–Se thin films from non-aqueous medium. *Thin Solid Films*, 1997, vol. 311, issue 1-2, pp. 114–118.
20. Virt I. S., Rudyj I. O., Kurilo I. V., Lopatynskyi I. Ye., Linnik L. F., Tetyorkin V. V., Potera P., Luka G. Properties of Sb<sub>2</sub>S<sub>3</sub> and Sb<sub>2</sub>Se<sub>3</sub> thin films obtained by pulsed laser ablation. *J. Semicond.*, 2013, vol. 47, issue 7, pp. 1003-1007.
21. Kamruzzaman M., Liu Chaoping, Farid Ul Islam A.K.M., Zapien J.A. A comparative study on the electronic and optical properties of Sb<sub>2</sub>Se<sub>3</sub> thin film. *Semiconductors/physics of the solid state*. 2017, vol. 51, no.12, pp. 1673-1681.
22. Chen S., Qiao X., Zheng Z., Cathelinard M., Ma H., Fan X., Zhang X. Enhanced electrical conductivity and photoconductive properties of Sn-doped Sb<sub>2</sub>Se<sub>3</sub> crystals. *J. Mater. Chem. C*, 2018, vol. 6, issue 24, pp. 6465-6470.
23. Dahshan A., Aly K.A. Optical constants of new amorphous As–Ge–Se–Sb thin films. *J. Acta Mater.*, 2008, vol. 56, pp. 4869–4875.
24. Zhang L., Li Y., Li Ch., Chen Q., Zhen Z., Jiang X., Zhong M., Zhang F., Zhu H. Scalable Low-Bandgap Sb<sub>2</sub>Se<sub>3</sub> Thin-Film Photocathodes for Efficient Visible-Near-Infrared Solar Hydrogen Evolution. *ACS Nano*, 2017, vol. 11, no.12, pp. 12753–12763.
25. Li Z., Chen X., Zhu H., Chen J., Guo Y., Zhang C., Zhang W., Niu X., Mai Y. Sb<sub>2</sub>Se<sub>3</sub> thin film solar cells in substrate configuration and the back contact selenization. *Sol. Energy Mater. Sol. C.*, 2017, vol. 161, pp. 190–196.
26. Abd El-Salam F., Afify M.A., Abd El-Wahabb E. Thickness and temperature dependence of the electrical resistivity of amorphous Sb<sub>2</sub>Se<sub>3</sub> films. *Vacuum*, 1993, vol. 44, no.10, pp. 1009 – 1013.
27. Tiwari K.J., Ren M.Q., Vajandar S.K., Osipowicz T., Subrahmanyam A., Malar P. Mechanochemical bulk synthesis and e-beam growth of thin films of Sb<sub>2</sub>Se<sub>3</sub> photovoltaic absorber. *Sol. Energy*, 2018, vol. 160, pp. 56–63.
28. El-Sayad E.A., Moustafa A.M., Marzouk S.Y. Effect of heat treatment on the structural and optical properties of amorphous Sb<sub>2</sub>Se<sub>3</sub> and Sb<sub>2</sub>Se<sub>2</sub>S thin films. *Physica B*, 2009, vol. 404, pp. 1119–1127.
29. Hu X., Tao J., Chen S., Xue J., Weng G., Kaijiang, Hu Z., Jiang J., Chen S., Zhu Z., Chu J., Improving the efficiency of Sb<sub>2</sub>Se<sub>3</sub> thin-film solar cells by post annealing treatment in vacuum condition. *Sol. Energy Mater. Sol. C.*, 2018, vol. 187, pp. 170-175.
30. Liu X., Chen C., Wang L., Zhong J., Luo M., Chen J., Xue D.J., Li D., Zhou Y., Tang J. Improving the performance of Sb<sub>2</sub>Se<sub>3</sub> thin film solar cells over 4% by controlled addition of oxygen during film deposition. *Prog. Photovoltaics: Research and Applications*, 2015, vol. 23, pp. 1828–1836.
31. Li Z., Zhu H., Guo Y., Niu X., Chen X., Zhang C., Zhang W., Liang X., Zhou D., Chen J., Mai Y. Efficiency enhancement of Sb<sub>2</sub>Se<sub>3</sub> thin-film solar cells by the co-evaporation of Se and Sb<sub>2</sub>Se<sub>3</sub>. *Appl. Phys. Express*, 2016, vol. 9, no. 5, 052302. [https:doi:10.7567/APEX.9.052302](https://doi:10.7567/APEX.9.052302)
32. Calixto-Rodriguez M., García H.M., Nair M.T.S., Nair P.K. Antimony Chalcogenide/Lead Selenide Thin Film Solar Cell with 2.5% Conversion Efficiency Prepared by Chemical Deposition. *ECS J. Solid State Sci. Technol.*, 2013, vol. 2, no. 4, pp. Q69-Q73.
33. Liu X.S., Chen J., Luo M., Leng M.Y., Xia Z., Zhou Y., Qin S.K., Xue D.J., Lv L., Huang H., Niu D.M., Tang J. Thermal evaporation and characterization of Sb<sub>2</sub>Se<sub>3</sub> Thin film for substrate Sb<sub>2</sub>Se<sub>3</sub>/CdS solar cells. *ACS Appl. Mater. Interfaces*, 2014, vol. 6, no. 13, pp. 10687–10695.
34. Ma X., Zhang Z., Wang X., Wang S., Xu F., Qian Y. Large-scale growth of wire-like

- Sb<sub>2</sub>Se<sub>3</sub> microcrystallines via PEG-400 polymer chain-assisted route. *J. Crys. Growth*, 2004, vol. 263, pp. 491–497.
35. Xie Q., Liu Z., Shao M., Kong L., Yu W., Qian Y. Polymer-controlled growth of Sb<sub>2</sub>Se<sub>3</sub> nanoribbons via a hydrothermal process. *J. Crys. Growth*, 2003, vol. 252, pp. 570–574.
36. Fernández A.M., Merino M.G. Preparation and characterization of Sb<sub>2</sub>Se<sub>3</sub> thin films prepared by electrodeposition for photovoltaic applications. *Thin Solid Films*, 2000, vol. 66, pp. 202–206.
37. Costa M.B., Lucas F.W.S., Mascaro L.H. Electrodeposition of Fe-doped Sb<sub>2</sub>Se<sub>3</sub> thin films for photoelectrochemical applications and study of the doping effects on their properties. *J. Solid State Electrochem.*, 2018, vol. 22, no. 5, pp. 1557–1562.
38. Desai J.D., Ganage N.K. Electrodeposition of Sb<sub>2</sub>Se<sub>3</sub> thin films from alkalin bath. *Bull. Electrochem.*, 1999, vol. 15, pp. 318–320.
39. Jiang L., Chen J., Wang Y., Sun K., Liu F., Lai Y. Graphene-Sb<sub>2</sub>Se<sub>3</sub> thin films photoelectrode synthesized by in situ electrodeposit ion. *J. Mater. Lett.*, 2018, vol. 224, pp. 109–112.
40. Kwon Y.H., Kim Y.B., Jeong M., Do H.W., Cho H.K., Lee J.Y. Crystal growth directioncontrolled antimony selenide thin film absorbers produced using an electrochemical approach and intermediat ethermal Treatment . *Sol. Energy Mater. Sol. C.*, 2017, vol. 172, pp. 11–17.
41. Kim Y.B., Kim J.S., Baek S.K., Yun Y.D., Cho S.W., Jung S.H., Cho H.K. Electrochemical surface charge-inversion from semi-insulating Sb<sub>2</sub>Se<sub>3</sub> photoanodes and abrupt photocurrent generation for water splitting. *Energy and Envi ron. Sci.*, 2018, vo l. 11, pp. 2540–2549.
42. Lai Y., Chen Z., Han C., Jiang L., Liu F., Li J., Liu Y. Preparation and characterization of Sb<sub>2</sub>Se<sub>3</sub> thin films by electrodeposition and annealing treatment. *Appl. Surf. Sci.*, 2012, vol. 261, pp. 510–514.
43. Ngo T.T., Chavhan S., Kosta I., Miguel O., Grande H.J., Tena-Zaera R. Electrodeposition of Antimony Selenide Thin Films and Application in Semiconductor Sensitized Solar Cells. *ACS Appl. Mater. Interfaces*, 2014, vol. 6, no. 4, pp. 2836–2841.
44. Torane A.P., Bhosale C.H. Preparation and characterization of electrodeposited Sb<sub>2</sub>Se<sub>3</sub> thin films from non-aqueous media. *J. Phys. Chem. Solids*, 2002, vol. 63, pp. 1849 – 1833.
45. Shi X., Zhang X., Tian Y., Shen C., Wang C., Gao H.J. Electrodeposition of Sb<sub>2</sub>Se<sub>3</sub> on indium-doped tin oxides substrate: Nucleation and growth. *Appl. Surf. Sci.*, 2012, vol. 258, pp. 2169–2173.
46. Chen Y., Wang L., Pradel A., Merlen A., Ribes M., Record M.C. Underpotential deposition of selenium and antimony on gold. *J. Solid State Electrochem.*, 2015, vol. 19, pp. 2399–2411.
47. Prabhakar R.R., Septina W., Siol S., Moehl T., Wick-Joliat R., Tilley S.D. PhotocorrosionResistant Sb<sub>2</sub>Se<sub>3</sub> Photocathodes with Earth Abundant MoS<sub>x</sub> Hydrogen Evolution Catalyst. *J. Mater. Chem. A*, 2017, vol. 44, no. 5, pp. 23139–23145.
48. Shi X., Zhang X., Ma C., Wang C. Kinetic studies of under potential deposition of antimony on Se-modified Au electrode. *J. Solid State Electrochem.*, 2010, vol. 14, pp. 93–99.
49. Tang A., Long M., He Z. Electrodeposition of Sb<sub>2</sub>Se<sub>3</sub> on TiO<sub>2</sub> nanotube arrays for catalytic reduction of p-nitrophenol. *J. Electrochim. Acta*, 2014, vol. 146, pp. 346–352.
50. Costa M.B., Lucas F.W.S., Mascaro L.H. Thermal Treatment Effects on Electrodeposited Sb<sub>2</sub>Se<sub>3</sub> Photovoltaic Thin Films. *J. Chem. ElectroChem.* 2017, vol. 4, issue 10, pp. 2507 – 2514.
51. Torane A.P., Rajpure K.Y., Bhosale C.H. Preparation and characterization of electrodeposited Sb<sub>2</sub>Se<sub>3</sub> thin films. *Mater. Chem. Phys.*, 1999, vol. 61, pp. 219–222.
52. Lai Y., Chen Z., Han C., Jiang L., Liu F., Li J., Liu Y. Preparation and characterizat ion o f Sb<sub>2</sub>Se<sub>3</sub> thin films by electrodeposit ion and annealing treatment. *Applied Surface Science*, 2012, vol. 261, pp. 510-514.
53. Park J., Yang W., Oh Y., Tan J., Lee H., Boppella R., Moon J. Efficient Solar to Hydrogen Conversion from Neutral Electrolytes using Morphology-Controlled

- Sb<sub>2</sub>Se<sub>3</sub> Light Absorber. *ACS Energy Lett.*, 2019, vol. 4, no. 2, pp. 517–526.
54. Majidzade V.A., Aliyev A.Sh., Guliyev P.H., Babanly D.M. Electrodeposition of the Sb<sub>2</sub>Se<sub>3</sub> thin films on various substrates from the tartaric electrolyte. *J. Electrochem. Sci. Eng.*, 2020, vol. 10, no. 1, pp. 1-9 <http://dx.doi.org/10.5599/jese.676>
55. Majidzade V.A., Guliyev P.H., Aliyev A.Sh., Elrouby M., Tagiyev D.B. Electrochemical Characterization and Electrode kinetics for Antimony Electrodeposition from its Oxychloride Solut ion in the Presence of Tartaric Acid. *J. Mol. Struc.*, 2017, vol. 1136, pp. 7-13.
56. Majidzade V.A., Aliyev A.Sh., Guliyev P.H., Babayev Y.N., Elrouby M., Tagiyev D.B. Electrochemical behavior of selenite ions in tartaric electrolytes. *J. Electrochem. Sci. Eng.*, 2018, vol. 8, n0. 3, pp. 197-204.
57. Majidzade V.A. Effect of various factors on the composit ion of electrolytic thin films Sb-Se. *Chemical Problems*, 2018, vol.16, no. 3, pp. 331-336.
58. Guo H., Chen Z., Wang X., Cang Q., Jia X., Ma C., Yuan N., Ding J. Enhancement in the Efficiency of Sb<sub>2</sub>Se<sub>3</sub> Thin-Film Solar Cells by Increasing Carrier Concentration and Inducing Columnar Growth of the Grains. *Solar RRL*, 2019, vol. 3, issue 3, article no. 1800224, <https://doi.org/10.1002/solr.201800224>
59. Birkett M., Linhart W.M., Stoner J., Phillips L.J., Durose K., Alaria J., Major J.D., Kudrawiec R., Veal T.D. Band gap temperature-dependence of close-space sublimation grown Sb<sub>2</sub>Se<sub>3</sub> by photo-reflectance. *J. APL Mater.*, 2018, vol. 6, 084901 <https://doi.org/10.1063/1.5027157>.
60. Kolay A., Kokal R.K., Kalluri A., Macwan I., Patra P.K., Ghosal P., Deepa M. New Antimony Selenide / Nickel Oxide Photocathode Boosts the Efficiency of Graphene Quantum Dots Co-sensitized Solar Cell. *ACS Appl. Mater. Interfaces*, 2017, vol. 9, no. 40, pp. 34915–34926.
61. Liu X., Xiao X., Yang Y., Xue D.J., Li D.B., Chen C., Lu S., Gao L., He Y., Beard M.C., Wang G., Chen S., Tang J. Enhanced Sb<sub>2</sub>Se<sub>3</sub> solar cell performance through theoryguided defect control. *Prog. in photovoltaics: Research and Applications*, 2017, vol. 25, no. 10, pp. 861-870.
62. Lu S., Zhao Y., Chen C., Zhou Y., Li D., Li K., Chen W., Wen X., Wang C., Kondrotas R., Lowe N., Tang J. Sb<sub>2</sub>Se<sub>3</sub> Thin-Film Photovoltaics Using Aqueous Solution Sprayed SnO<sub>2</sub> as the Buffer Layer. *Adv. Electron. Mater.*, 2017, vol. 4, 1700329 <https://doi.org/10.1002/aelm.201700329> 63. Wang X., Tang R., Wu C., Zhu C., Chen T. Development of antimony sulfide– selenide Sb<sub>2</sub>(S,Se)<sub>3</sub>-based solar cells. *J. Energy Chem.*, 2017, vol. 27, no. 3, pp. 713-721.
64. Kumar P., Thangaraj R. Structural phase transit ions and optical contrast in amorphous Sb<sub>2</sub>Se<sub>3</sub>: Sn Films. *J. Chalcogen. Lett.*, 2010, vol. 7, no. 8, pp. 509-513.
65. Das S., Kambo S., Sirohi A., Vasdev A., Gayen S., Guptasarma P., Sheet G. Discovery of highly spin-polarized conducting surface states in the strong spin-orbit coupling semiconductor Sb<sub>2</sub>Se<sub>3</sub>. *Phys. Rev. B*, 2018, vol. 97, pp. 1-5.
66. Browning R., Kuperman N., Moon B., Solanki R. Atomic Layer Growth of InSe and Sb<sub>2</sub>Se<sub>3</sub> Layered Semiconductors and Their Heterostructure. *J. Electron.*, 2017, vol. 27, no. 6, pp. 1-10.
67. Chen C., Yang Y., Bobela D.C., Lu S., Zeng K., Yang B., Gao L., Beard M.C., Tang J. Characterization of Basic Physical Properties of Sb<sub>2</sub>Se<sub>3</sub> and it s relevance for photovoltaics. *Front. Optoelectron.*, 2017, vol. 10, no. 1, pp. 18–30.
68. Yang W., Ahn J., Oh Y., Tan J., Lee H., Park J., Kwon H.C., Kim J., Jo W., Kim J., Moon J. Adjusting the Anisotropy of 1D Sb<sub>2</sub>Se<sub>3</sub> Nanostructures for Highly Efficient Photoelectrochemical Water Splitting. *J. Energy Mater.*, 2018, vo. 8, 1702888 <https://doi.org/10.1002/aenm.201702888>
69. Yang W., Lee S., Kwon H.C., Tan J., Lee H., Park J., Oh Y., Choi H., Moon J. TimeResolved Observations of PhotoGenerated Charge-Carrier Dynamics in Sb<sub>2</sub>Se<sub>3</sub> Photocathodes for Photoelectrochemical Water Splitting. *J. ACS Nano*, 2018, vol. 12, pp. 11088–11097.
70. Iovu M.S., Vasiliev I.A., Colomeico E.P. Negative photoconductivity of amorphous Sb<sub>2</sub>Se<sub>3</sub> and Sb<sub>2</sub>Se<sub>3</sub>:Sn films. *Int. J.*

- Electron.*, 1981, vol. 51, no. 6, pp. 735–742.
71. Iovu M.S., Colomeico E.P., Vasiliev I.A. Photoconductivity of amorphous Sb<sub>2</sub>Se<sub>3</sub> and Sb<sub>2</sub>Se<sub>3</sub>:Sn thin films. *Chalcogen. Lett.*, 2007, vol. 4, no. 9, pp. 109 – 113.
72. Chen Z., Guo X., Guo H., Ma C., Qiu J., Yuan N., Ding J. Fabrication of a semi-transparent thin-film Sb<sub>2</sub>Se<sub>3</sub> solar cell. *Mater. Lett.*, 2019, vol. 236, pp. 503-505.
73. Hu X., Tao J., Weng G., Jiang J., Chen S., Zhu Z., Chu J. Investigation of electrically-active defects in Sb<sub>2</sub>Se<sub>3</sub> thin-film solar cells with up to 5.91% efficiency via admittance spectroscopy. *Sol. Energy Mater. Sol. C.*, 2018, vol. 186, pp. 324–329.
74. Aoki T., Shimada H. Reversible photoinduced changes of electronic transport in narrow-gap amorphous Sb<sub>2</sub>Se<sub>3</sub>. *Phys. Rev. B*, 1999, vol. 59, no. 3, pp. 1579-1581.
75. Zhang X., Korolkov I., Fan B., Cathelinaud M., Ma H., Adam J.-L., Merdrignac O., Calvez L., Lhermite H., Brizoual L.L., Pasquinelli M., Simon J.-J. Chalcogenide glass-ceramic with self-organized heterojunct ions: application to photovoltaic solar cells. *EPJ Photovolt.*, 2018, vol. 9, no.3, pp. 1-6. <https://doi.org/10.1051/epjpv/2018002>
76. Tao J., Hu X., Xue J., Wang Y., Weng G., Chen S., Zhu Z., Chu J. Investigation of electronic transport mechanisms in Sb<sub>2</sub>Se<sub>3</sub> thin-film solar cells. *Sol. Energy Mater. Sol. C.*, 2019, vol. 197, pp. 1–6.
77. Zayed H.A., Abo-Elsoud A.M., Ibrahim A.M., Kenawy M.A. The composition dependence of the optical constants in amorphous Sb<sub>x</sub>Se<sub>1-x</sub> thin films. *Thin Solid Films*, 1994, vol. 247, pp. 94-97.
78. Vadapoo R., Krishnan S., Yilmaz H., Marin C. Self-standing nanoribbons of antimony selenide and antimony sulfide with well-defined size and band gap. *J. Nanotechnol.*, 2011, vol. 22, no.17, 175705. https: doi: 10.1088/0957-4484/22/17/175705
79. Carey J.J., Allen J.P., Scanlon D.O., Watson G.W. The electronic structure of the antimony chalcogenide series: prospects for optoelectronic applications. *J. Solid State Chem.*, 2014, vol. 213, pp. 116–125.
80. Tan J., Yang W., Oh Y., Lee H., Park J., Boppella R., Kim J., Moon J. Fullerene as a Photoelectron Transfer Promoter Enabling Stable TiO<sub>2</sub>-Protected Sb<sub>2</sub>Se<sub>3</sub> Photocathodes for Photo Electrochemical Water Splitting. *Adv. Energy Mater.*, 2019, 1900179. <https://doi.org/10.1002/aenm.201900179>
81. Lee H., Yang W., Tan J., Oh Y., Park J., Moon J. Cu-doped NiO<sub>x</sub> as Effective Hole-Selective Layer for High-Performance Sb<sub>2</sub>Se<sub>3</sub> Photocathode for Photoelectrochemical Water Splitting. *ACS Energy Lett.*, 2019, vol. 4, no. 5, pp. 995–1003.
82. Majidzade V.A., Aliyev A.Sh., Qasimoglu I., Quliyev P.H., Tagiyev D.B. Electrical Properties of Electrochemically Grown Thin Sb<sub>2</sub>Se<sub>3</sub> Semiconductor Films. *Inorg. Mater.*, 2019, vol. 55, no. 10, pp. 979–983.

## ***Sb<sub>2</sub>Se<sub>3</sub> ƏSASINDA GÜNƏŞ ELEMENTLƏRİ: ONLARIN ALINMASI VƏ XASSƏLƏRİ***

*Vüsalə A. Məcidzadə*

*AMEA-nin akad. M.Nağıyev adına Kataliz və Qeyri-iüzvi Kimya İnstitutu,  
AZ 1143, H. Cavid pr.113, Bakı, Azərbaycan, e-mail:vuska\_80@mail.ru*

*Məlum olduğu kimi, Sb<sub>2</sub>Se<sub>3</sub> optik və elektrik xüsusiyyətlərinə görə günəş elementlərində effektiv udma qabiliyyətinə malik yarımkənarıcı təbəqədir. Son illərdə Sb<sub>2</sub>Se<sub>3</sub> əsasında nazik təbəqəli günəş elementlərində enerjinin çevrilmə effektivliyi tədricən artmaqdadır. Ona görə də təqdim edilən iş müxtəlif sulu və qeyri-sulu elektrolitlərdən Sb-Se nazik təbəqələrinin müxtəlif texnologiyalarla hazırlanmasına dair geniş ədəbiyyat icmanın nəzərdən keçirilməsinə və habelə onların quruluşunun bəzi optik və elektrik xüsusiyyətlərinin öyrənilməsinə həsr edilmişdir. Müxtəlif elektrodlarda birgə çökmə potensialı pH-dan, temperaturdan,*

*elektrolitin tərkibindən və uyğun olaraq sürmə və selenium qatılından asılı olaraq öyrənilmişdir. Müxtəlif atmosferlərdə  $Sb_2Se_3$ -nin kristal əmələgətirməsinə termiki emalın təsiri də tədqiq edilmişdir.*

**Açar sözlər:** elektroçökmə; nazik təbəqələr; sürmə selenid; kristalların quruluşları; sulu və susuz elektrolitlər

## **СОЛНЕЧНЫЕ ЭЛЕМЕНТЫ НА ОСНОВЕ $Sb_2Se_3$ : ПОЛУЧЕНИЕ И СВОЙСТВА**

*Вюсала А. Меджидзаде*

*Институт Катализа и Неорганической Химии им. акад. М. Нагиева Национальной АН  
Азербайджана, AZ 1143, Баку, пр. Г. Джавида, 113, e-mail: [vuska\\_80@mail.ru](mailto:vuska_80@mail.ru)*

Как известно,  $Sb_2Se_3$  является эффективным поглощающим слоем в солнечных элементах, благодаря своим оптическим и электрическим свойствам. В последние годы эффективность преобразования энергии тонкопленочных солнечных элементов на основе  $Sb_2Se_3$  постепенно повышается. Поэтому статья посвящена литературному обзору исследований различных технологий получения тонкопленочной системы  $Sb$ - $Se$  из различных водных и неводных электролитов, а также и изучению ее структуры, некоторых оптических и электрических свойств. Рассмотрены результаты исследований потенциалов совместного осаждения на различных субстратах в зависимости от температуры, pH и состава электролита, источников сурьмы и селена, а также влияния термической обработки на зарождение кристаллов  $Sb_2Se_3$  в различных атмосферах.

**Ключевые слова:** электроосаждение, тонкие пленки, селенид сурьмы, структура кристаллов, водные и неводные растворы